Microvascular Research 151 (2024) 104608

Contents lists available at ScienceDirect

Microvascular Research

journal homepage: www.elsevier.com/locate/ymvre

# Handheld vital microscopy for the identification of microcirculatory alterations in cervical intraepithelial neoplasia and cervical cancer

Y.P. Latul [a,b,*], C. Ince [c], N.E. van Trommel [d], A. van den Brandhof-van den Berg [a], J.P.W. R. Roovers [a,b,e], A.W. Kastelein [a,b]

[a] Amsterdam University Medical Centers location University of Amsterdam, Dept. of Obstetrics and Gynecology, Meibergdreef 9, Amsterdam, the Netherlands
[b] Amsterdam Reproduction and Development Research Institute, Amsterdam, the Netherlands
[c] Department of Intensive Care, Erasmus MC, University Medical Center, Rotterdam, the Netherlands
[d] The Netherlands Cancer Institute (NKI), Department of Gynaecologic Oncology, Antoni van Leeuwenhoek Hospital (AvL), Amsterdam, the Netherlands
[e] Bergman Clinics, Department of Gynaecology & Sexology, Bergman Vrouwenzorg, Amsterdam, the Netherlands

ARTICLE INFO

*Keywords:*
Cervix uteri
Uterine cervical dysplasia
Uterine cervical neoplasms
Microvessels
Handheld vital microscopy
Incident dark field imaging
Angioarchitecture

ABSTRACT

*Background:* Ninety percent of cervical cancer (CC) diagnoses and deaths occur in low and middle-income countries (LMICs). Especially in these countries, where human and material resources are limited, there is a need for real-time screening methods that enable immediate treatment decisions (i.e., 'see and treat').
*Objective:* To evaluate whether handheld vital microscopy (HVM) enables real-time detection of microvascular alterations associated with cervical intraepithelial neoplasia (CIN) and CC.
*Methods:* A cross-sectional study was conducted in an oncologic hospital and outpatient clinic, and included ten healthy controls, ten women with CIN, and ten women with CC. The microvasculature was assessed in four quadrants of the uterine cervix using HVM. The primary outcome was the presence of abnormal angioarchitecture (AA). Secondary outcomes included capillary loop density (CD), total vessel density (TVD), functional capillary density (FCD), and the proportion of perfused vessels (PPV).
*Results:* 198 image sequences of the cervical microvasculature were recorded. Compared to healthy controls, significantly more abnormal image sequences were observed in women with high-grade CIN (11 % vs. 44 %, $P < 0.001$) and women with CC (11 % vs. 69 %, $P < 0.001$). TVD, FCD, and PPV were lower in women with CIN and CC.
*Conclusions:* HVM enables easy, real-time, non-invasive assessment of cervical lesions through the detection of microvascular alterations. Thereby, HVM potentially provides an opportunity for point-of-care screening, which may enable immediate treatment decisions (see and treat) and reduce the number of unnecessary surgical interventions.

## 1. Introduction

Worldwide, approximately 604,000 women are diagnosed with and 342,000 women die from cervical cancer (CC) every year (Sung et al., 2021). In high-income countries (HICs), the implementation of well-organized screening programs has drastically decreased the prevalence of CC through the detection and treatment of CC precursors (cervical intraepithelial neoplasia (CIN)) (Sung et al., 2021). Such screening programs require infrastructure and extensive human and material resources, which are lacking in low and middle-income countries (LMICs) (Xue et al., 2020). Consequently, 90 % of CC diagnoses and deaths occur in LMICs (Sung et al., 2021). In these countries, there is a need for real-time screening methods to enable immediate treatment decisions (see and treat) without time- and resource-consuming histology or repeated visits (Xue et al., 2020).

Currently, treatment decisions are based on histologic examination of colposcopy-guided biopsies. Low-grade lesions (CIN 1) are likely to regress spontaneously and high-grade lesions (CIN 2 and 3) have a higher risk of progression to CC (Perkins et al., 2020; Tainio et al., 2018). Consequently, CIN 1 is managed expectantly with close observation,

* Corresponding author at: Amsterdam University Medical Centers location University of Amsterdam, Dept. of Obstetrics and Gynecology, Meibergdreef 9, Amsterdam, the Netherlands.
*E-mail address:* y.p.latul@amsterdamumc.nl (Y.P. Latul).

https://doi.org/10.1016/j.mvr.2023.104608
Received 7 August 2023; Received in revised form 7 September 2023; Accepted 7 September 2023
Available online 9 September 2023

whereas CIN 3 is generally treated surgically (large loop excision of the transformation zone (LLETZ)) (Perkins et al., 2020). In the case of CIN 2, expectant management is increasingly considered to be the preferred option, especially in younger patients, since LLETZ but also repeated biopsies are associated with an increased risk of premature birth in future pregnancies (Loopik et al., 2021).

To reduce the number of unnecessary biopsies and enable immediate diagnosis, a real-time, non-invasive method for assessing CIN is desirable (Xue et al., 2020). It has long been established that CIN and CC gradually increase vascular density and alter vascular morphology (Stafl and Mattingly, 1975). Clinicians evaluate such vascular alterations (mosaicism, punctation, and atypical vessels) during colposcopy (Perkins et al., 2020). However, colposcopy is highly subjective and requires experienced operators and subsequent invasive biopsies for histologic evaluation. A non-invasive, detailed, and objective method for assessing cervical microvasculature could enable in vivo diagnosis. Hand-held vital microscopy (HVM) is such a method that has been used to quantify microcirculatory alterations in a large range of diseases, including malignancies, and has demonstrated high consistency among multiple observers (i.e., high *intraclass correlation coefficient* for scoring vaginal microcirculatory parameters) (Ince et al., 2018; Mathura et al., 2001; Kastelein et al., 2020). Incident dark field (IDF) imaging is the latest generation of HVM, which we have demonstrated to be feasible for the assessment of cervical microvasculature in healthy volunteers (Latul et al., 2021).

In the current study, we use HVM to assess the cervical microvasculature in patients with CIN and CC to evaluate whether HVM enables real-time detection of microvascular alterations associated with CIN and CC. A non-invasive, real-time method to assess CIN has several potential advantages, including 1) enabling real-time screening, 2) reducing the number of invasive biopsies, and 3) possibly predicting the malignant potential of CIN lesions and thereby reducing the risk of under- and overtreatment.

## 2. Methods

This cross-sectional study was conducted in the Antoni van Leeuwenhoek Hospital (the Netherlands Cancer Institute, METC18.0773) and Bergman Clinics Vrouw (outpatient clinic for women's care). The objective was to evaluate whether HVM enables the detection of microvascular changes occurring with CIN and CC.

### 2.1. Participants and setting

We aimed to include ten women in each of the following groups: healthy controls, high-grade CIN (CIN 2+), and CC. Exclusion criteria included: 1. extensive cardiovascular disease (e.g., untreated hypertension), 2. systemic illnesses with the potential to affect the microcirculation (e.g., untreated diabetes mellitus), and 3. use of medication that could potentially affect the microcirculation (e.g., anticoagulants, systemic anti-inflammatory, or immunosuppressive agents). As part of standard care, CIN and CC were histologically evaluated through biopsies or excision after HVM.

### 2.2. Handheld vital microscopy

The cervical microvasculature was assessed using HVM (CytoCam, Braedius Medical, Huizen, the Netherlands), a lightweight (120 g) handheld pen-like device (length 220 mm, diameter 23 mm, tip diameter 5 mm) that uses green light epi-illumination (wavelength 530 nm, pulse time 2 ms) to create a real-time image of the functional microcirculation (pixel size 1.4 μm, field of view 1.16 mm × 1.55 mm, magnification factor 4) (Ince et al., 2018). HVM measurements were performed in a gynecological chair (control and CIN groups) or operating theatre (CC group) in the lithotomy position before any cervical intervention. The cervix was visualized using a speculum and wiped clean from mucus, lubricant, or blood if necessary. The CytoCam was gently placed onto the cervix with a sterile disposable cap. Focus and contrast were manually optimized and image sequences of 3 s were recorded in four quadrants of the cervix, i.e., at 12, 3, 6, and 9 o'clock. If the squamocolumnar junction (SCJ) was visible, both squamous and columnar epithelium were imaged (resulting in eight image sequences). Image acquisition was performed by researchers with extensive training and experience with the CytoCam (YPL, ABB, and AWK).

### 2.3. Image analysis

Recorded image sequences were saved on a hard drive and analyzed both qualitatively and quantitatively. Quality assessment was performed using Massey's scoring system, which includes six quality parameters, i.e., illumination, duration, focus, content, stability, and pressure (Massey and Shapiro, 2016). As we did not want to exclude image sequences containing capillary loops, we changed the parameter 'content' to artifacts only. If an image sequence did not meet the other parameters, it was excluded from quantitative analysis.

#### 2.3.1. Angioarchitecture

Two blinded researchers classified the microvascular patterns (angioarchitecture, AA) according to Weber's classification; score 1 represents capillary loops, score 2 both capillary loops and vascular networks, and score 3 vascular networks without capillary loops (Fig. 1) (Latul et al., 2021). Images that could not be scored according to this AA classification were classified as 'abnormal' (primary outcome). Differences between the two assessors were resolved by consensus.

#### 2.3.2. Quantitative microcirculatory parameters

For image sequences displaying AA score 1, the capillary loop density (CD, capillary loops per square millimeter, cpll/mm$^2$) was calculated manually (Latul et al., 2021). Quantitative analysis of AA score 3 was performed using Automated Vascular Analysis 3.2 (AVA, Microvision, the Netherlands), resulting in the parameters: total vessel density (TVD, the total length of vessels per square millimeter, mm/mm$^2$), functional capillary density (FCD, perfused vessels per square millimeter, mm/mm$^2$), and the proportion of perfused vessels (PPV, %) (Dobbe et al., 2008). As no validated method exists for the analysis of AA score 2, these image sequences were excluded from quantitative analysis. Image sequences classified as 'abnormal' were analyzed according to their best resemblance (i.e., CD when most resemblance to score 1, and AVA when most resemblance to score 3).

### 2.4. Statistical analysis

Descriptive statistics were used to display baseline characteristics and microcirculatory parameters. Shapiro-Wilk testing was used to assess the normality of numerical data. For categorical variables, between-group (healthy vs. CIN vs. CC) analysis was performed using Fisher's exact test. For normally distributed numerical data, the one-way ANOVA with Tukey's (equal variances) or Games-Howell (no equal variances) post hoc test was used. Non-normally distributed numerical data were compared using the Kruskal-Wallis test with the post hoc Mann-Whitney-*U* test. Image sequences demonstrating normal vs. abnormal AA were compared using the independent samples *t*-test or Mann-Whitney U test, depending on the variables' distribution. A two-sided $P < 0.05$ was considered statistically significant.

## 3. Results

### 3.1. Patient characteristics

Patient and image characteristics of 30 included women are presented in Table 1. None of the included participants had relevant comorbidity. Women with CC were significantly older and had a higher

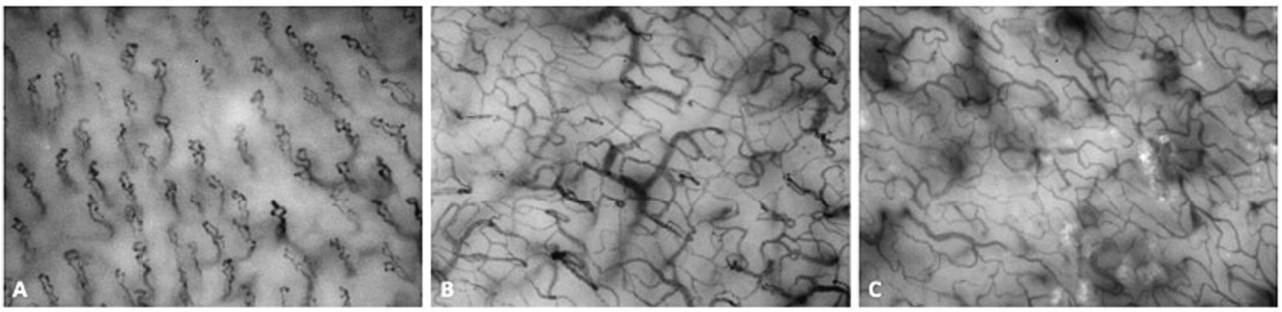


**Fig. 1.** Angioarchitecture according to Weber's classification. Screenshots of handheld vital microscopy of the uterine cervix obtained in healthy controls. A: Weber score 1 (capillary loops), B: Weber score 2 (combination of capillary loops and vascular network), and C: Weber score 3 (vascular network). Each image represents a field of view of 1.16 × 1.55 mm.

**Table 1**
Patient characteristics and microcirculatory parameters. Comparison between healthy controls, women with high-grade CIN, and women with cervical cancer. Bold values indicate statistical significance. Mean (95 % CI) reported for BMI, TVD, FCD, and CD. Median (IQR) reported for age, alcohol, and PPV. Abbreviations: n = number of women, N = number of images, CIN = cervical intraepithelial neoplasia, BMI = body mass index, SCJ = squamocolumnar junction, hr-HPV = high-risk human papillomavirus, SCC = squamous cell carcinoma, AC = adenocarcinoma, ASC = adenosquamous carcinoma, AA = angioarchitecture, TVD = total vessel density, FCD = functional capillary density, PPV = proportion of perfused vessels, CD = capillary loop density, cpll = capillary loop count.

| Patient characteristics | Healthy controls ($n$ = 10) | High-grade CIN (n = 10) | $P$ value * | Cervical cancer (n = 10) | $P$ value ** | $P$ value *** |
|---|---|---|---|---|---|---|
| Age (years)[a] | 32 (27–74) | 30 (29–33) | 0.85 | 45 (39–51) | 0.20 | **<0.01** |
| BMI (kg/m$^2$)[b] | 22.9 (21.2–24.6) | 21.1 (19.7–22.4) | 0.29 | 24.5 (21.9–27.0) | 0.41 | **<0.05** |
| Smoking (n, %)[c] | 1 (10 %) | 4 (40 %) | 0.30 | 2 (20 %) | 1.00 | 0.63 |
| Alcohol (u/week)[a] | 0 (0–7.75) | 4.5 (2.75–7) | 0.18 | 2.5 (0.75–4.75) | 0.31 | 0.21 |
| SCJ visible (n, %)[c] | 4 (40 %) | 6 (60 %) | 0.66 | 2 (20 %) | 0.63 | 0.17 |
| hr-HPV + (n, %) | – | 10 (100 %) | – | 10 (100 %) | – | – |
| Histopathological diagnosis | – | CIN 2: 3 (30 %)<br>CIN 3: 7 (70 %) | – | SCC: 6 (60 %)<br>AC: 3 (30 %)<br>ASC: 1 (10 %) | – | – |

| Image characteristics | Healthy controls ($N$ = 47) | High-grade CIN ($N$ = 62) | $P$ value * | Cervical cancer ($N$ = 54) | $P$ value ** | $P$ value *** |
|---|---|---|---|---|---|---|
| Abnormal AA (N, %)[c] | 5 (11 %) | 27 (44 %) | **<0.001** | 37 (69 %) | **<0.001** | **<0.01** |
| Patients with ≥1 abnormal AA (n, %)[c] | 5 (50 %) | 10 (100 %) | **<0.05** | 10 (100 %) | **<0.05** | – |
| Patients with >1 abnormal AA (n, %)[c] | 0 (0 %) | 8 (80 %) | **<0.001** | 10 (100 %) | **<0.001** | 0.47 |
| TVD (mm/mm$^2$)[d] | 12.29 (11.17–13.41) | 9.89 (8.06–11.72) | 0.07 | 8.51 (7.68–9.33) | **<0.001** | 0.34 |
| FCD (mm/mm$^2$)[d] | 12.23 (11.11–13.36) | 9.23 (7.21–11.26) | **<0.05** | 6.82 (5.59–8.06) | **<0.001** | 0.13 |
| PPV (%)[a] | 100 (100–100) | 98.58 (80.91–100) | **<0.01** | 89.60 (50.87–100) | **<0.001** | 0.08 |
| CD (cpll/mm$^2$)[b] | 33.23 (28.25–38.20) | 30.93 (25.11–36.75) | 0.81 | 46.43 (38.21–54.65) | **<0.05** | **<0.05** |

[a] Kruskall-Wallis, post hoc Mann-Whitney-$U$ test.
[b] One-way ANOVA, post hoc Tukey.
[c] Fisher's exact test.
[d] ANOVA, post hoc Games-Howell.
* Healthy vs. CIN.
** Healthy vs. CC.
*** CIN vs. CC.

BMI than women with high-grade CIN (Table 1). Healthy controls above 30 years of age participated in the Dutch national screening program for CC and did not have prior cervical dysplasia. Of the healthy controls outside the screening window (30–60 years of age), no recent cervical smear was available, but no signs or symptoms of cervical pathology were present. Of the women with high-grade CIN, three had CIN 2 and seven had CIN 3 (Table 1). Of the women with CC, six had squamous cell carcinoma (SCC), three had adenocarcinoma (AC) and one had adenosquamous carcinoma (ASC, Table 1).

### 3.2. Imaging characteristics

Measurements were well tolerated by patients with a maximum acquisition time of 4 min. A total of 198 image sequences were recorded of which 35 were excluded because of technical problems or insufficient quality. Of the remaining image sequences, 11 were excluded from quantitative analysis (CD or TVD, FCD, and PPV) because of an AA score of 2.

#### 3.2.1. Angioarchitecture

In women with CC, the majority of image sequences demonstrated a chaotic and heterogeneous AA (Fig. 2 and Video 1). Compared to healthy controls, significantly more abnormal image sequences were observed in women with high-grade CIN (11 % vs. 44 %, $P < 0.001$) and women with CC (11 % vs. 69 %, $P < 0.001$, Table 1). All women with CIN and CC had at least one abnormal image sequence (Table 1). None of the healthy controls had more than one abnormal image sequence, compared to 80 % of women with CIN and 100 % of women with CC (Table 1).

#### 3.2.2. Quantitative microcirculatory parameters

TVD, FCD, and PPV decreased with increasing dysplasia (Table 1). CD was higher in women with CC than in healthy controls and women with CIN (Table 1). Compared to image sequences with a normal AA,

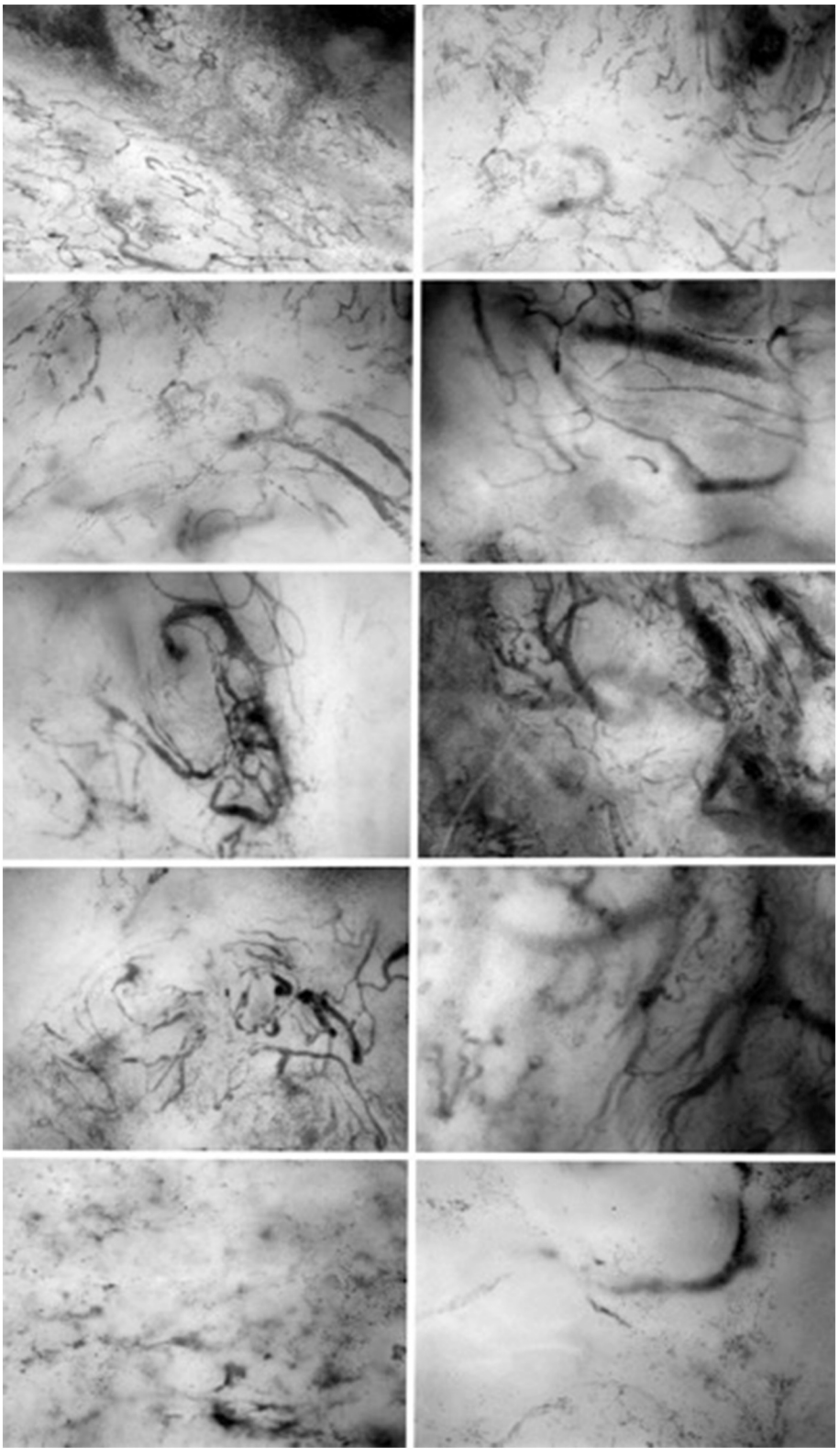

**Fig. 2.** Cervical microcirculation of women with cervical cancer. Screenshots of handheld vital microscopy demonstrate abnormal and heterogeneous microvessels, the absence of well-organized vascular patterns, extravascular erythrocytes, and avascular areas. Each image represents a field of view of 1.16 × 1.55 mm.

those with abnormal AA had a significantly lower TVD, FCD, and PPV (Supplementary Table 1).

## 4. Discussion

### *4.1. Main findings*

Using HVM, we demonstrated that the well-organized cervical

microvasculature of healthy controls is replaced by chaotic, heterogenous, and poorly perfused microvessels in women with CIN and CC. All women with CIN and CC had at least one image sequence with abnormal AA, suggesting that if no abnormal AA is observed, no CIN or CC is present.

### 4.2. Interpretation of results

The burden of CC remains a significant indicator of global health inequality. In 2018, the World Health Organization (WHO) emphasized the need for worldwide efforts to eliminate CC (World Health Organization, 2020). One of the key strategies is to ensure that 70 % of women aged 35 to 45 are screened, and 90 % of women receive appropriate management by 2030 (World Health Organization, 2020). High-income countries have witnessed a notable reduction in CC cases through well-established screening programs, which involve cervical smears, and – when necessary – colposcopy with subsequent biopsies for histologic evaluation (Sung et al., 2021). The decline in CC incidence in these countries can be attributed to the detection and effective treatment of CIN and thereby prevention of CC. However, such screening programs require infrastructure and experienced clinicians, which are lacking in LMICs, resulting in long delays between visits, loss of follow-up, and consequently unnecessary high prevalence and mortality of CC (Xue et al., 2020). Therefore, in low-resource settings, there is a need for affordable, real-time screening methods that do not require experienced clinicians, time-consuming histology, or repeated visits to enable immediate treatment decisions (see and treat) (Xue et al., 2020).

Early detection of human papillomavirus (HPV) infection is crucial for effective CC screening and prevention. Nearly all CC cases are caused by persistent high-risk HPV infection, and therefore, if no high-risk HPV is present, there is no indication for further diagnostics or interventions. Traditionally, HPV detection has been performed through cytology of clinician-collected cervical samples, which is time and resource-consuming. In LMICs, cervical cytology screening has not yet reached high population coverage (Petersen et al., 2022). Non-invasive self-sampling methods have emerged as promising alternatives for HPV detection (Arbyn et al., 2018; Arbyn et al., 2014). Additionally, advancements in molecular biology and diagnostic technologies have paved the way for non-invasive point-of-care testing (POCT) devices for HPV detection (Basak et al., 2021). Implementing self-sampling strategies combined with POCT has the potential to improve screening participation rates, particularly among underscreened populations, and increase the overall effectiveness of CC prevention programs.

However, the presence of high-risk HPV alone is not an indication for surgical intervention. Following high-risk HPV detection, the uterine cervix should be assessed to localize and grade cervical lesions to make treatment decisions. Currently, suspect lesions are evaluated through colposcopy and, when necessary, subsequent biopsies for histologic evaluation (WHO, 2003). Since colposcopy and pathology services are limited in LMICs, there is a need for alternative, affordable methods to assess the uterine cervix in real-time. Non-invasive imaging methods, such as high-resolution narrow band or multispectral endoscopy (Yu et al., 2020; Fujii et al., 2010), optical coherence tomography (Ren et al., 2021), high-resolution microendoscopy (Pierce et al., 2012; Quinn et al., 2012; Grant et al., 2017), telecentric lens optical imaging (Canpolat et al., 2022) and photoacoustic imaging (Peng et al., 2015) have emerged as valuable tools for CC screening, providing anatomical and functional information without the need for invasive procedures.

In a previous study, we demonstrated that HVM is a feasible method to assess the cervical microcirculation of healthy controls non-invasively in real-time (Latul et al., 2021). We demonstrated that unaffected uterine cervixes feature two distinct, well-organized microvascular patterns; i.e., capillary loops and vascular networks (Fig. 1) (Latul et al., 2021). In the current study, we demonstrated that microvascular alterations induced by CIN and CC can be detected using HVM (Fig. 2). It has long been established that CIN and CC induce cervical microvascular changes (Yetkin-Arik et al., 2021). Infection with high-risk HPV contributes to the formation of new blood vessels through a complex process involving oncoproteins E6 and E7, which results in the activation of vascular endothelial growth factor (VEGF) and consequently tumor angiogenesis (Yetkin-Arik et al., 2021; Pal and Kundu, 2020). Multiple histopathological studies have demonstrated regions of neovascularization directly underneath CIN lesions, and increasing microvessel density with increasing dysplasia (Smith-McCune, 1997; Guidi et al., 1995; Dobbs et al., 1997; Lee et al., 2002; Dellas et al., 1997; Tjalma et al., 1999; Smith-McCune and Weidner, 1994). Tumor angiogenesis has been correlated to poorer prognosis, underlining the relevance of microvascular assessment in diagnosing and treating CIN (Dellas et al., 1997).

Our results suggest that if no abnormal AA is observed using HVM, no high-grade CIN or CC is present. Future studies should evaluate whether this is also the case in a larger population. If that is the case, artificial intelligence (AI) should be incorporated to enable automated differentiation between normal and abnormal AA, which is currently still susceptible to interobserver variation. If AI successfully differentiates between healthy, CIN, and CC, this would facilitate immediate treatment decisions without the need for extensive human and material resources. This will be subject to future study.

### 4.3. Strengths and limitations

Strengths of our study include the fact that we incorporated a healthy control group, used a standardized imaging protocol, were blinded during image analysis, and incorporated both quantitative and qualitative outcome measures. Our study is limited by its small sample size and the fact that we did not differentiate between CIN 2 and 3. Limitations of HVM include imaging depth (maximum 300 μm) and field of view ($1.8mm^2$). However, since cervical dysplasia arises from the epithelium, this imaging depth should be sufficient for the assessment of CIN and CC. A larger field of view could make the assessment of the cervical surface quicker and easier. In our study, quantitative analysis was performed manually, which is time-consuming and delays the interpretation of quantitative outcome measures. The recent introduction of MicroTools, an advanced computer algorithm that enables instantaneous and automatic analysis and quantification of microcirculatory parameters, enables rapid assessment of these parameters (Hilty et al., 2019). Future studies should validate whether MicroTools could be applied to the uterine cervix.

### 4.4. Conclusions and clinical relevance

HVM enables easy, real-time, non-invasive screening of cervical lesions through the detection of microvascular alterations, which could facilitate immediate diagnosis and treatment (see and treat) and potentially reduce the number of unnecessary interventions and (at random) biopsies.

Supplementary data to this article can be found online at https://doi.org/10.1016/j.mvr.2023.104608.

## CRediT authorship contribution statement

**Y.P. Latul:** Formal analysis, Investigation, Data curation, Writing – original draft, Visualization. **C. Ince:** Conceptualization, Methodology, Writing – review & editing. **N.E. van Trommel:** Methodology, Writing – review & editing. **A. van den Brandhof-van den Berg:** Investigation, Writing – review & editing. **J.P.W.R. Roovers:** Conceptualization, Methodology, Writing – review & editing, Supervision. **A.W. Kastelein:** Conceptualization, Methodology, Investigation, Writing – review & editing, Supervision.

## Declaration of competing interest

Braedius Medical, a company owned by a relative of Dr. Ince, has developed CytoCam-IDF imaging used in this study. Dr. Ince has no financial relationship with Braedius Medical of any sort, i.e., never owned shares or received consultancy or speaker fees from Braedius Medical. Dr. Ince is CSO of Active Medical BV, Leiden, The Netherlands, a company that provides devices (OxyCam), software (MicroTools), education (Microcirculation Academy), and services related to clinical microcirculation. All other authors declare that they have no conflict of interest.

## Data availability

The data that support the findings of this study are available on request from the corresponding author.

## Acknowledgements

The authors thank all women that participated in this study, as well as Patricia Beemster (Bergman Clinics) for facilitating the study procedures. This research did not receive any specific grant from funding agencies in the public, commercial, or not-for-profit sectors. Materials were provided by Braedius Medical (Huizen, the Netherlands).

## References

Arbyn, M., Verdoodt, F., Snijders, P.J.F., et al., 2014. Accuracy of human papillomavirus testing on self-collected versus clinician-collected samples: a meta-analysis. Lancet Oncol. 15 (2), 172–183. https://doi.org/10.1016/S1470-2045(13)70570-9.

Arbyn, M., Smith, S.B., Temin, S., Sultana, F., Castle, P., 2018. Detecting cervical precancer and reaching underscreened women by using HPV testing on self samples: updated meta-analyses. BMJ 363, k4823. https://doi.org/10.1136/bmj.k4823.

Basak, M., Mitra, S., Agnihotri, S.K., et al., 2021. Noninvasive point-of-care nanobiosensing of cervical cancer as an auxiliary to pap-smear test. ACS Appl. Bio Mater. 4 (6) https://doi.org/10.1021/acsabm.1c00470.

Canpolat, M., Birge, Ö., Danışman, T., et al., 2022. The detection of cervical neoplasia via optical ımaging: a pilot clinical study. Arch. Gynecol. Obstet. 306 (2) https://doi.org/10.1007/s00404-021-06389-w.

Dellas, A., Moch, H., Schultheiss, E., et al., 1997. Angiogenesis in cervical neoplasia: microvessel quantitation in precancerous lesions and invasive carcinomas with clinicopathological correlations. Gynecol. Oncol. 67 (1), 27–33. https://doi.org/10.1006/gyno.1997.4835.

Dobbe, J.G.G., Streekstra, G.J., Atasever, B., van Zijderveld, R., Ince, C., 2008. Measurement of functional microcirculatory geometry and velocity distributions using automated image analysis. Med. Biol. Eng. Comput. 46 (7), 659–670. https://doi.org/10.1007/s11517-008-0349-4.

Dobbs, S.P., Hewett, P.W., Johnson, I.R., Carmichael, J., Murray, J.C., 1997. Angiogenesis is associated with vascular endothelial growth factor expression in cervical intraepithelial neoplasia. Br. J. Cancer 76 (11), 1410–1415.

Fujii, T., Nakamura, M., Kameyama, K., et al., 2010. Digital colposcopy for the diagnosis of cervical adenocarcinoma using a narrow band imaging system. Int. J. Gynecol. Cancer 20 (4). https://doi.org/10.1111/IGC.0b013e3181d98da9.

Grant, B.D., Fregnani, J.H.T.G., Possati Resende, J.C., et al., 2017. High-resolution microendoscopy: a point-of-care diagnostic for cervical dysplasia in low-resource settings. Eur. J. Cancer Prev. 26 (1) https://doi.org/10.1097/CEJ.0000000000000219.

Guidi, A.J., Abu-Jawdeh, G., Berse, B., et al., 1995. Vascular permeability factor (vascular endothelial growth factor) expression and angiogenesis in cervical neoplasia. J. Natl. Cancer Inst. 87 (16), 1237–1245.

Hilty, M.P., Guerci, P., Ince, Y., Toraman, F., Ince, C., 2019. MicroTools enables automated quantification of capillary density and red blood cell velocity in handheld vital microscopy. Commun. Biol. 2, 217. https://doi.org/10.1038/s42003-019-0473-8.

Ince, C., Boerma, E.C., Cecconi, M., et al., 2018. Second consensus on the assessment of sublingual microcirculation in critically ill patients: results from a task force of the European Society of Intensive Care Medicine. Intensive Care Med. 44 (3), 281–299. https://doi.org/10.1007/s00134-018-5070-7.

Kastelein, A.W., Vos, L.M.C., van Baal, J.O.A.M., et al., 2020. Poor perfusion of the microvasculature in peritoneal metastases of ovarian cancer. Clin. Exp. Metastasis. https://doi.org/10.1007/s10585-020-10024-4 (Published online February).

Latul, Y.P., Kastelein, A.W., Beemster, P.W.T., van Trommel, N.E., Ince, C., Roovers, J.P.W.R., 2021. Noninvasive, in vivo assessment of the cervical microcirculation using incident dark field imaging. Microvasc. Res. 135, 104145 https://doi.org/10.1016/j.mvr.2021.104145.

Lee, J.S., Kim, H.S., Jung, J.J., Lee, M.C., Park, C.S., 2002. Angiogenesis, cell proliferation and apoptosis in progression of cervical neoplasia. Anal. Quant. Cytol. Histol. 24 (2), 103–113.

Loopik, D.L., Van Drongelen, J., Bekkers, R.L.M., et al., 2021. Cervical intraepithelial neoplasia and the risk of spontaneous preterm birth: a Dutch population-based cohort study with 45,259 pregnancy outcomes. PLoS Med. 18 (6) https://doi.org/10.1371/journal.pmed.1003665.

Massey, M.J., Shapiro, N.I., 2016. A guide to human in vivo microcirculatory flow image analysis. Crit. Care 20, 35. https://doi.org/10.1186/s13054-016-1213-9.

Mathura, K.R., Bouma, G.J., Ince, C., 2001. Abnormal microcirculation in brain tumours during surgery. Lancet 358 (9294), 1698–1699. https://doi.org/10.1016/S0140-6736(01)06722-8.

Pal, A., Kundu, R., 2020. Human papillomavirus E6 and E7: the cervical cancer hallmarks and targets for therapy. Front. Microbiol. 10. https://doi.org/10.3389/fmicb.2019.03116.

Peng, K., He, L., Wang, B., Xiao, J., 2015. Detection of cervical cancer based on photoacoustic imaging - the in-vitro results. Biomed. Opt. Express 6 (1). https://doi.org/10.1364/boe.6.000135.

Perkins, R.B., Guido, R.S., Castle, P.E., et al., 2020. 2019 ASCCP risk-based management consensus guidelines for abnormal cervical cancer screening tests and cancer precursors. J. Low. Genit. Tract Dis. 24 (2), 102–131. https://doi.org/10.1097/LGT.0000000000000525.

Petersen, Z., Jaca, A., Ginindza, T.G., et al., 2022. Barriers to uptake of cervical cancer screening services in low-and-middle-income countries: a systematic review. BMC Womens Health 22 (1). https://doi.org/10.1186/s12905-022-02043-y.

Pierce, M.C., Guan, Y.Y., Quinn, M.K., et al., 2012. A pilot study of low-cost, high-resolution microendoscopy as a tool for identifying women with cervical precancer. Cancer Prev. Res. 5 (11) https://doi.org/10.1158/1940-6207.CAPR-12-0221.

Quinn, M.K., Bubi, T.C., Pierce, M.C., Kayembe, M.K., Ramogola-Masire, D., Richards-Kortum, R., 2012. High-resolution microendoscopy for the detection of cervical neoplasia in low-resource settings. PloS One 7 (9). https://doi.org/10.1371/journal.pone.0044924.

Ren, C., Zeng, X., Shi, Z., et al., 2021. Multi-center clinical study using optical coherence tomography for evaluation of cervical lesions in-vivo. Sci. Rep. 11 (1) https://doi.org/10.1038/s41598-021-86711-3.

Smith-McCune, K., 1997. Angiogenesis in squamous cell carcinoma in situ and microinvasive carcinoma of the uterine cervix. Obstet. Gynecol. 89 (3), 482–483.

Smith-McCune, K.K., Weidner, N., 1994. Demonstration and characterization of the angiogenic properties of cervical dysplasia. Cancer Res. 54 (3), 800–804.

Stafl, A., Mattingly, R.F., 1975. Angiogenesis of cervical neoplasia. Am. J. Obstet. Gynecol. 121 (6), 845–852.

Sung, H., Ferlay, J., Siegel, R.L., et al., 2021. Global Cancer statistics 2020: GLOBOCAN estimates of incidence and mortality worldwide for 36 cancers in 185 countries. CA Cancer J. Clin. 71 (3) https://doi.org/10.3322/caac.21660.

Tainio, K., Athanasiou, A., Tikkinen, K.A.O., et al., 2018. Clinical course of untreated cervical intraepithelial neoplasia grade 2 under active surveillance: systematic review and meta-analysis. BMJ 360, k499. https://doi.org/10.1136/bmj.k499.

Tjalma, W., Sonnemans, H., Weyler, J., van Marck, E., van Daele, A., van Dam, P., 1999. Angiogenesis in cervical intraepithelial neoplasia and the risk of recurrence. Am. J. Obstet. Gynecol. 181 (3), 554–559.

WHO, 2003. Colposcopy and treatment of cervical intraepithelial neoplasia: a beginners' manual. In: Colposcopy and Treatment of Cervical Intraepithelial Neoplasia: A Beginners' Manual, 1 (Cin 1).

World Health Organization, 2020. Global Strategy to Accelerate the Elimination of Cervical Cancer as a Public Health Problem, Vol 2.

Xue, P., Ng, M.T.A., Qiao, Y., 2020. The challenges of colposcopy for cervical cancer screening in LMICs and solutions by artificial intelligence. BMC Med. 18 (1) https://doi.org/10.1186/s12916-020-01613-x.

Yetkin-Arik, B., Kastelein, A.W., Klaassen, I., et al., 2021. Angiogenesis in gynecological cancers and the options for anti-angiogenesis therapy. Biochim. Biophys. Acta Rev. Cancer 1875 (1), 188446. https://doi.org/10.1016/j.bbcan.2020.188446.

Yu, W., Long, C., Zhu, T., Zhu, H., Han, Z., Li, F., 2020. High resolution multispectral endoscopy significantly improves the diagnostic accuracy of cervical intraepithelial lesions. J. Obstet. Gynaecol. Res. 46 (6) https://doi.org/10.1111/jog.14241.